

Signatures of Discontinuity in the Exchange-Correlation Energy Functional Derived from the Subband Electronic Structure of Semiconductor Quantum Wells

S. Rigamonti and C. R. Proetto
 Centro Atómico Bariloche and Instituto Balseiro,
 8400 S.C. de Bariloche, Río Negro, Argentina
 (Dated: October 13, 2017)

The discontinuous character of the exact exchange-correlation (xc) energy functional of Density Functional Theory is shown to arise naturally in the subband spectra of semiconductor quantum wells. Using an *ab-initio* xc functional, including exchange exactly and correlation in an exact partial way, a discontinuity appears in the xc potential, each time a subband becomes slightly occupied. Exchange and correlation give opposite contributions to the discontinuity, with correlation overcoming exchange. The jump in the intersubband energy is in excellent agreement with experimental data.

Density Functional Theory (DFT) has become the standard calculational tool in physics and quantum chemistry for the study of atomic, molecular, and solid state systems. The theory is based in the Hohenberg-Kohn theorems[1], that place the ground-state electron density as the basic variable and provides a variational principle for its calculation. Kohn and Sham (KS) showed how the problem of variational minimization for the density could be exactly mapped to one of non-interacting particles in an effective potential, which contains only one non-trivial component: the exchange-correlation (xc) contribution[1]. DFT, however, gives no clue on how to proceed for its practical calculation. Naturally a lot of attention has been devoted to the development of better xc energy functionals; KS introduced the highly successful Local Density Approximation (LDA), which is widely employed nowadays, along with the improvements born from it (such as the Generalized Gradient Approximation or GGA, meta-GGA, etc.)[2]. The work described here is motivated by this fundamental need of better approximations for the xc energy functional[3], using as "laboratory" to test the accuracy of the approximations the subband electronic structure of the quasi two-dimensional electron gases (*2DEG*) formed at the interface between two dissimilar semiconductors, such as GaAs and AlGaAs. In this Letter we show that at the one-subband \rightarrow two-subband quantum well (QW) transition ($1S \rightarrow 2S$), the xc potential behaves discontinuously, with exchange and correlation giving opposite contributions (i.e., competing) to the discontinuity. The intersubband energy, which also jumps abruptly at the transition, is in excellent agreement with experiments.

Our model system is a semiconductor modulation-doped QW grown epitaxially, as shown in the upper inset of Fig. 1. Assuming translational symmetry in the ($x-y$) plane (area A), and proposing accordingly a solution of the type $\phi_{i\mathbf{k}\sigma}(\boldsymbol{\rho}, z) = e^{i\mathbf{k}\cdot\boldsymbol{\rho}}\xi_i^\sigma(z)/\sqrt{A}$, with $\boldsymbol{\rho}$ the in-plane coordinate, the zero temperature ground-state electron density can be obtained by solving a set of effective one-dimensional KS equations of the form:

$$\left[-\frac{1}{2} \frac{\partial^2}{\partial z^2} + V_{KS}^\sigma(z) \right] \xi_i^\sigma(z) = \varepsilon_i^\sigma \xi_i^\sigma(z), \quad (1)$$

where effective atomic units have been used. $\xi_i^\sigma(z)$ is the wavefunction for electrons in subband i ($i = 1, 2, \dots$), spin σ ($\sigma = \uparrow, \downarrow$), and eigenvalue ε_i^σ . The local (multiplicative) KS potential $V_{KS}^\sigma(z)$ is the sum of several terms: $V_{KS}^\sigma(z) = V_{ext}(z) + V_H(z) + V_{xc}^\sigma(z)$. $V_{ext}(z)$ is given by the epitaxial potential plus an external electric field. $V_H(z)$ is the Hartree potential. Within DFT, $V_{xc}^\sigma(z) = A^{-1} \delta E_{xc} / \delta n_\sigma(z)$. Departing from the main stream in most applications of KS-DFT, our xc energy functional is an explicit functional of the whole set of ε_i^σ 's and ξ_i^σ 's, $E_{xc} = E_{xc}[\{\varepsilon_i^\sigma, \xi_i^\sigma\}]$, but an implicit (in general unknown) functional of the spin-resolved density $n_\sigma(z)$. The zero-temperature 3D electron density is $n_\sigma(z) = \sum_{\varepsilon_i^\sigma < \mu} (\mu - \varepsilon_i^\sigma) |\xi_i^\sigma(z)|^2 / 2\pi$, with μ the chemical potential. By assuming a paramagnetic situation, we drop the spin index σ from this point.

The xc energy functional E_{xc} for our *2DEG* has been generated by Görling-Levy (GL) perturbation theory where the correlation energy is expanded in a series[4],

$$E_{xc}[\{\varepsilon_i, \xi_i\}] = E_x[\{\varepsilon_i, \xi_i\}] + \sum_{n=2}^{\infty} E_c^{GL(n)}[\{\varepsilon_i, \xi_i\}], \quad (2)$$

which is truncated at its leading contribution $n = 2$. E_x in equation above is the exact exchange energy, known explicitly as a Fock integral of the KS occupied orbitals. Its multi-subband explicit expression is given by Eq.(38) in Ref.[5] (denoted as I below). The terms $E_c^{GL(n)}$ can be found explicitly[4]. At difference with E_x , however, they depend both on occupied and an infinite number of unoccupied subbands. Their numerical evaluation is in consequence rather expensive. The explicit expression for $E_c^{GL(2)}$ for our semiconductor QW system is given by Eqs.(32) and (33) of I. A similar correlation energy functional has been used in Refs.[6] and [7] for the case of atoms, with mixed results. As shown here, Eq.(2) seems much more promising for the *2DEG*[8].

The next non-trivial problem is the evaluation of $V_{xc}(z)$, given the already quoted implicit dependence of E_{xc} on $n(z)$ in Eq. (2). The procedure for dealing with implicit functionals relies on the use of the chain rule for

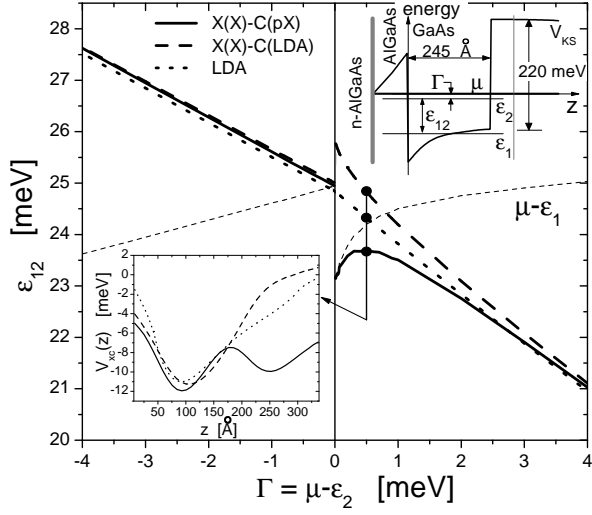


Figure 1: Ground-state \rightarrow first-excited intersubband energy ε_{12} as a function of Γ . Negative (positive) values of Γ correspond to the $1S$ ($2S$) regime. Upper inset: schematic view of our model for the modulation-doped QW. A charge-transfer field along z is induced by a distant metallic plate (thin vertical line at right). If the metallic plate is positively (negatively) charged, more (less) electrons are transferred towards the well from an ionized donor impurities region (thick vertical stripe at left), which acts as a particle reservoir fixing the chemical potential μ . Lower inset: $V_{xc}(z)$ in the same three different approximations as for ε_{12} ($\Gamma = 0.5$ meV). The QW extends from $z = 50$ Å to $z = 295$ Å.

functional derivatives as follows [4]:

$$V_{xc}(z) = \frac{1}{A} \frac{\delta E_{xc}}{\delta n(z)} = \frac{1}{A} \int \frac{\delta E_{xc}}{\delta V_{KS}(z')} \frac{\delta V_{KS}(z')}{\delta n(z)} dz'. \quad (3)$$

To proceed with the calculation of $V_{xc}(z)$ directly from Eq.(3), we use a numerical method devised and explained in detail in I. Eqs.(1)-(3) should be iterated until full self-consistency is achieved.

We present in Fig. 1 the intersubband energy spacing $\varepsilon_{12} \equiv \varepsilon_2 - \varepsilon_1$, as a function of $\Gamma \equiv \mu - \varepsilon_2$, for three approximations for E_{xc} : LDA, exact-exchange plus LDA for correlation [X(X)-C(LDA)], and X(X) plus partial exact-correlation ($E_c^{GL(2)}$), denoted as X(X)-C(pX). Note that while the resulting ε_{12} are quite similar in the whole $1S$ regime, and in the $2S$ regime with sizable occupation of the second subband, noticeable differences arise in the limit of small second subband occupancy. Starting with the X(X)-C(LDA) approximation, ε_{12} shows an exchange-driven abrupt *positive* jump at the $1S \rightarrow 2S$ [9]. The inclusion of C(pX) overcomes the X(X)-C(LDA) positive jump, resulting now in a *negative* jump in ε_{12} , until it levels with the other results at finite second subband fillings. LDA

is in between the two kind of discontinuities at $\Gamma = 0$, showing only a discontinuity in the derivative. The lower inset shows the corresponding $V_{xc}(z)$ in the relevant QW region. $V_{xc}(z)$ as resulting from X(X)-C(LDA) builds a barrier just where most of the weight of $\xi_2(z)$ is concentrated, pushing ε_2 upwards under small occupancy of the second subband, and leaving ε_1 more or less unaltered; this explains the discontinuous positive behavior of ε_{12} . It is also physically reasonable: by blocking the occupation of the second subband, the exchange energy is optimized, as the intrasubband exchange is larger than the intersubband exchange. The $V_{xc}(z)$ in the X(X)-C(pX) behaves just in the opposite way: it develops a deep well just after the transition, inducing an abrupt decrease of ε_2 at more or less constant ε_1 . This explains the abrupt decrease of ε_{12} in this case. The behavior has again a simple physical explanation: by inducing the occupancy of the second subband, $V_{xc}(z)$ promotes a spatial separation between electrons in both subbands, decreasing correlation and its associated repulsive energy. With respect to the $V_{xc}(z)$ resulting from LDA, it shows the expected smooth and continuous behavior at the transition.

Besides these fully numerical results, we provide below an analytical derivation of the results of Fig. 1, for $\Gamma \simeq 0$. In the limit $|\Gamma| \rightarrow 0$, E_{xc} can be approximated as

$$E_{xc}^{(\alpha)} = P_{xc}^{(\alpha)} + \Gamma Q_{xc}^{(\alpha)}, \quad (4)$$

with $\alpha = 1S, 2S$. Here, $P_{xc}^{(1S)} = E_{xc}(\Gamma \rightarrow 0^-)$, $P_{xc}^{(2S)} = E_{xc}(\Gamma \rightarrow 0^+)$, $Q_{xc}^{(1S)} = dE_{xc}/d\Gamma|_{0^-}$, $Q_{xc}^{(2S)} = dE_{xc}/d\Gamma|_{0^+}$. By inspection of the explicit expressions for E_x and $E_c^{GL(2)}$ given in I, it is concluded that $P_{xc}^{(1S)} = P_{xc}^{(2S)} = P_{xc}$, and that $Q_{xc}^{(1S)} \neq Q_{xc}^{(2S)}$. In words, for a fixed set of $\varepsilon_{i \neq 2}$'s and $\xi_i(z)$'s, the xc functional is continuous at the $1S \rightarrow 2S$, but its derivative is discontinuous. The explicit expressions for P_{xc} , $Q_{xc}^{(1S)}$ and $Q_{xc}^{(2S)}$ are not needed for the present derivation. Inserting Eq.(4) in Eq.(3) we obtain,

$$V_{xc}^{(\alpha)}(z) = \int \left[\frac{\delta P_{xc}}{\delta V_{KS}(z')} - Q_{xc}^{(\alpha)} |\xi_2(z')|^2 \right] \chi_{\alpha}^{-1}(z', z) dz'. \quad (5)$$

Here, we have defined $\chi_{\alpha}^{-1}(z, z') \equiv \delta V_{KS}(z)/\delta n_{\alpha}(z')$, and used the result $\delta\Gamma/\delta V_{KS}(z) = -\delta\varepsilon_2/\delta V_{KS}(z) = -|\xi_2(z)|^2$, obtained by first-order perturbation theory. We have also neglected a term linear in Γ , which becomes arbitrarily small in the limit $\Gamma \rightarrow 0$. In the limit $\Gamma \rightarrow 0^+$, the density response function[5] becomes

$$\chi_{2S}(z, z') = \chi_{1S}(z, z') - |\xi_2(z)\xi_2(z')|^2/\pi. \quad (6)$$

Its inverse can be calculated by using the Sherman-Morrison technique[10]. We obtain

$$\chi_{2S}^{-1}(z, z') = \chi_{1S}^{-1}(z, z') + D(z)D(z')/[\pi(1 + \lambda)], \quad (7)$$

where $D(z) = \int \chi_{1S}^{-1}(z, x) |\xi_2(x)|^2 dx$, and $\lambda = -\pi^{-1} \int D(x) |\xi_2(x)|^2 dx$. As we can see from Eq.(7),

$\chi_{2S}^{-1}(z, z')$ is discontinuous at the $1S \rightarrow 2S$ transition, such as it is $\chi_{2S}(z, z')$ of Eq.(6). Using now Eq.(5) for $\alpha = 1S, 2S$ and exploiting the explicit expression for $\chi_{2S}^{-1}(z, z')$ as given by Eq.(7), we arrive at the result

$$\Delta V_{xc}(z) \equiv V_{xc}^{(2S)}(z) - V_{xc}^{(1S)}(z) = C_{xc}D(z)/(1 + \lambda), \quad (8)$$

with $C_{xc} = \langle V_{xc}^{(1S)} \rangle_2 / \pi - \Delta Q_{xc}$, $\langle \mathcal{O} \rangle_i = \int dx |\xi_i(x)|^2 \mathcal{O}(x)$ and $\Delta Q_{xc} = Q_{xc}^{(2S)} - Q_{xc}^{(1S)}$. Eq.(8) is an important result, which shows explicitly how the functional dependence on z of the xc potential changes discontinuously at the $1S \rightarrow 2S$ transition. For an arbitrary subband transition $NS \rightarrow (N+1)S$ it can be shown that the result of Eq.(8) is still valid, with the replacements $1 \rightarrow N$ and $2 \rightarrow N+1$ in Eqs.(4)-(8). Equation 8 follows rigorously from Eq.(4), and then it is important to discuss its validity. In writing Eq.(4) we have implicitly made a "frozen" assumption, by taking the same set of wavefunctions $\xi_i(z)$ and energies ε_i both for $\Gamma \rightarrow 0^-$ and $\Gamma \rightarrow 0^+$. In the language of the numerical self-consistent calculations leading to Fig. 1, it is as if the results for the $1S$ case in the limit $\Gamma \rightarrow 0^-$ were extrapolated to the $2S$ $\Gamma \rightarrow 0^+$ case, by performing a single iteration loop towards full self-consistency. This "frozen" result for the xc energy functional is illustrated in Fig. 2 by the straight lines, separating exchange ($P_x + \Gamma Q_x^\alpha$) from correlation ($P_c + \Gamma Q_c^\alpha$). Besides, if the approximation for E_{xc} is such that $\Delta V_{xc}(z) \neq 0$ (that is, if $C_{xc} \neq 0$), it is clear that the self-consistent iteration loop will lead to a further discontinuity in the xc energy functional itself right at the $1S \rightarrow 2S$ transition ($\Gamma = 0$), once convergence has been reached. These fully self-consistent results correspond to the thick full (E_x) and dashed ($E_c^{GL(2)}$) lines in Fig. 2. On the other side, if the approximation for E_{xc} is such that $C_{xc} = 0$, no discontinuity of the type of Eq.(8) exists for $V_{xc}(z)$ before or after self-consistency is achieved, which in turn implies the continuity of E_{xc} . Our $E_{xc} = E_{xc}[\{\varepsilon_i^\sigma, \xi_i^\sigma\}]$ is such that $C_{xc} \neq 0$; local (LDA) approximations for E_{xc} yield $C_{xc} = 0$.

For further insight, the constant C_{xc} can be separated conveniently in its exchange and correlation components $C_n = \langle V_n^{(1S)} \rangle_2 / \pi - \Delta Q_n$, with $n = x, c$. The analysis of the results shown in Fig. 2 leads to the conclusion that $C_x < 0$ and $C_c > 0$, considering that $D(z) < 0$ (see inset in Fig. 2). Qualitatively, this happens in the following way: *a*) in the exchange case, $\langle V_x^{(1S)} \rangle_2$ is large and negative (see inset Fig. 2), while $-\Delta Q_x$ is a relatively small positive magnitude, resulting in $C_x < 0$; *b*) in the correlation case, $\langle V_c^{(1S)} \rangle_2$ is a very small quantity (see inset Fig. 2), while $-\Delta Q_c$ is a relatively large positive number, yielding a $C_c > 0$. The net result is that correlation overcomes exchange ($C_{xc} = C_x + C_c > 0$), and $\Delta V_{xc}(z)$ has a negative contribution resulting in the right attractive well shown in the lower inset of Fig. 1. It is important to note that this overcoming of correlation on exchange happens even when $|E_c^{GL(2)}| \ll |E_x|$ (Fig. 2). However, as Eq.(8) clearly shows, not only the magnitude of the xc

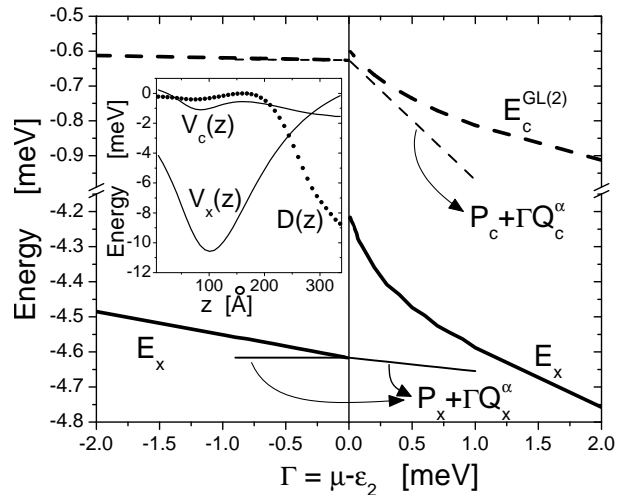


Figure 2: Full lines: E_x in the "frozen" (thin line) and self-consistent (thick line) approaches; dashed lines: $E_c^{GL(2)}$ in the "frozen" (thin line) and self-consistent (thick line) approaches. Note the cut in the vertical scale. Inset: exchange and correlation potentials (full lines) and function $D(z)$ (dotted line, arbitrary units) for $\Gamma = -0.01$ meV.

energy functional matters (represented by the $\langle V_{xc}^{(1S)} \rangle_2$ contribution), but also the respective derivatives (represented by the ΔQ_{xc} term). This exemplifies quite vividly the potential danger of neglecting correlation against exchange at the threshold of a subband transition, under the argument that the correlation energy is much smaller than the exchange energy.

Is there any experimental evidence of this type of discontinuities in semiconductor QW's? The answer is yes. We reproduce as an inset in the upper panel of Fig. 3 the experimental values for the subband densities n_1 and n_2 , plotted as a function of the Fermi level measured from the top of the valence band[11]. The data have been obtained from a quantitative analysis of photoluminescence line shapes. It is seen that when the Fermi level touches the bottom of the second subband, the electron density n_2 jumps from zero to a finite value ranging from 3×10^{10} to 8×10^{10} cm^{-2} , depending on temperature[11]. The electron density of the lowest subband, in contrast, increases slightly but smoothly with voltage, suggesting that the external electric field couples essentially to the $1S$ occupation, which seems quite plausible as it is the subband with the largest occupation. This motivates us to redraw the results for ε_{12} of Fig. 1 as a function of $\mu - \varepsilon_1$, in the lower panel of Fig. 3. Clearly the theoretical n_1 , n_2 , and ε_{12} vs. $\mu - \varepsilon_1$ agree quite well with the experimental data, both qualitatively and quantitatively. For instance, the theoretical value for the decreasing jump in ε_{12} at $\mu - \varepsilon_1 \simeq 25$ meV, amounts to about 3.3 meV, in excellent agreement with the 3.5 meV jump estimated

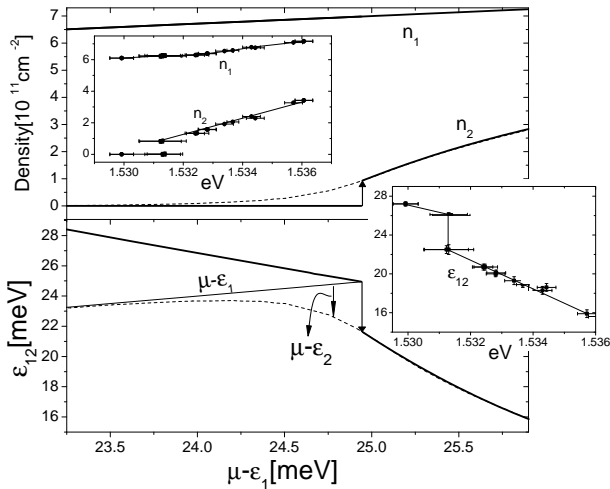


Figure 3: Thick full lines: Ground and first-excited subband densities n_1 and n_2 (upper panel) and intersubband transition energy ε_{12} (lower panel) as a function of $\mu - \varepsilon_1$. Dashed lines: n_2 and ε_{12} corresponding to a continuous filling of the first-excited subband, as in Fig. 1. Insets: experimental data from Ref.[11].

from experiment.

The results presented in this work are intimately related to the issue of the derivative discontinuity of ensemble DFT[12]. Among the many important consequences derived from this extension of DFT to fractional particle number, maybe the most important one in the field of solid state physics has been the realization that the true gap of semiconductors is not given by the KS one-particle gap[13]. Instead, the true gap is given by the sum of the

KS gap, plus the so-called xc discontinuity, Δ_{xc} . Continuum approximations to xc energy functionals, including all currently widely used LDA's and GGA's, fail to produce the correct value for Δ_{xc} , resulting in an important underestimation of the fundamental band-gap of most semiconductors and insulators. In a very recent work, Grüning *et al.* have clarified the theoretical situation, obtaining very good agreement between experimental and theoretical band gaps of Si, LiF, and Ar[14], by using an orbital based correlation energy functional corresponding to a dynamical screening of the Coulomb interaction (GW approximation). It was found that Δ_{xc} contributes as much as 30% – 50% to the energy gap. Their results, for a different type of systems, are fully consistent with ours.

In conclusion, the intrinsic discontinuity of the xc energy functional has been obtained entirely within a DFT framework, for a realistic system. We have shown that the xc energy functional generated by second-order Görling-Levy perturbation theory for the $2DEG$ has many of the properties of the exact functional. The main finding is that at the $1S \rightarrow 2S$ transition, the KS xc potential and the associated intersubband transition energies behave discontinuously, with x and c giving opposite contributions (i.e. competing) to the discontinuity, and with correlation overcoming exchange. Very good qualitative and quantitative agreement is obtained with experiments.

This work was partially supported by CONICET under grant PIP 5254 and the ANPCyT under PICT 03-12742. SR acknowledges financial support from CNEA-CONICET. CRP is a fellow of CONICET.

-
- [1] R. G. Parr and W. Yang, *Density Functional Theory of Atoms and Molecules*, (Oxford University Press, New York, 1989); R. M. Dreizler and E. K. U. Gross, *Density Functional Theory* (Springer-Verlag, Heidelberg, 1990).
- [2] J. Tao *et al.*, Phys. Rev. Lett. **91**, 146401 (2003).
- [3] A. E. Mattsson, Science **298**, 759 (2002).
- [4] A. Görling and M. Levy, Phys. Rev. B **47**, 13105 (1993); *ibid.*, Phys. Rev. A **52**, 4493 (1995).
- [5] S. Rigamonti and C. R. Proetto, Phys. Rev. B **73**, 235319 (2006). As the calculations of this work were restricted to the simpler $1S$ regime, *none* of the findings of the present work concerning the $1S \rightarrow 2S$ transition were considered. There is also an important difference from the technical point of view: the calculation of $E_c^{GL(2)}$ in a situation with two (or more) occupied subbands is far more complicated and numerically demanding than the $1S$ case, due to the presence in the many-subband case of four Fermi disk intersecting integrals, whose numerical evaluation becomes quite involved.
- [6] P. Mori-Sánchez, Q. Wu, and W. Yang, J. Chem. Phys. **123**, 062204 (2005).
- [7] H. Jiang and E. Engel, J. Chem. Phys. **123**, 224102 (2005).
- [8] As is well known, $E_c^{GL(2)}$ diverges in the long-wavelength limit for the case of the homogeneous $3D$ electron gas[15]. In contrast, this contribution is finite for the strict $2D$ homogeneous electron gas[16]. Our QW system is much closer to the $2D$ than to the $3D$ limit (corresponding to a very large number of occupied subbands). It seems then quite plausible that the perturbative expansion of Eq.(2) be much better convergent for the $2DEG$ than for the $3DEG$. From a practical point of view, evidence on this stems from the fact that the self-consistent loop among Eqs.(1)-(3) is robust and free from the instabilities found in Refs.[6] and [7].
- [9] S. Rigamonti, C. R. Proetto, and F. A. Reboredo, Europhys. Lett. **70**, 116 (2005).
- [10] W. H. Press *et al.*, in *Numerical Recipes* (Cambridge University Press, NY, 1992).
- [11] A. R. Goñi *et al.*, Phys. Rev. B **65**, 121313(R) (2002).
- [12] J. P. Perdew *et al.*, Phys. Rev. Lett. **49**, 1691 (1982).
- [13] J. P. Perdew and M. Levy, Phys. Rev. Lett. **51**, 1884 (1983); L. J. Sham and M. Schlüter, Phys. Rev. Lett. **51**, 1888 (1983). Note the similarity between Eq.(12) of the

latter work for the semiconductor band-gap discontinuity, and our Eq.(8) for the discontinuity of the xc potential at the $1S \rightarrow 2S$ transition.

- [14] M. Grüning, A. Marini and A. Rubio, J. Chem. Phys. **124**, 154108 (2006).
- [15] D. Pines, *Elementary Excitations in Solids* (Benjamin, New York, 1964).
- [16] A. K. Rajagopal and J. C. Kimball, Phys. Rev. B **15**, 2819 (1977); A. Ishihara and L. Ioriatti, *ibid.* **22**, 214 (1980).